An Approach for Characterizing the Frequency Response of Sampling-Oscilloscopes Using a Large-Signal Network Analyzer

Alirio S. Boaventura[#^1], Dylan F. Williams[#2], Paul D. Hale[#], Gustavo Avolio[$3]
[#]Communications Technology Laboratory, National Institute of Standards and Technology, USA
[^]Department of Physics, University of Colorado Boulder, USA
[$]Anteverta-mw, The Netherlands
[1]aliriodejesus.soaresboaventura@nist.gov, [2]dylan.williams@nist.gov, [3]gustavo@anteverta-mw.com

***Abstract*—We propose an approach for characterizing the complex frequency response of sampling oscilloscopes using a calibrated large-signal network analyzer (LSNA) and a broadband pulse source. First, we perform a full wave-parameter calibration of the LSNA using its internal continuous wave (CW) sources. Then, we replace the internal CW sources with an external broadband pulse source and measure it with the calibrated LSNA and oscilloscope connected to the LSNA test port. The complex frequency response of the oscilloscope's sampler is derived in the frequency domain as the ratio of the oscilloscope signal spectrum to the calibrated LSNA signal spectrum. We achieve less than 0.7 dB amplitude and 5 degrees phase difference up to 45 GHz between the proposed LSNA calibration and previous NIST electro-optic sampling (EOS) characterization of the same sampler.**

***Keywords*—Sampling-oscilloscope characterization, large-signal network analysis, standard transfer.**

I. Introduction

There has been a growing interest in the use of sampling oscilloscopes for microwave applications [1]-[3], due to their flexibility, low cost and increasing bandwidths. However, at microwave frequencies, oscilloscopes must be corrected for imperfections such as jitter, time-base distortion, impedance mismatch and frequency response [1].

The frequency response is typically characterized using an electro-optic sampling (EOS)-characterized high-speed pulse source [4]-[6]. This source is measured by the oscilloscope and the frequency response is derived by deconvolving the known reference signal from the measured signal. The deconvolution is usually performed in the frequency domain by dividing the measured signal spectrum by the reference signal spectrum, yielding the scope response.

In [7], we compared waveform measurements made simultaneously with an LSNA and a sampling oscilloscope, both calibrated to the same reference plane. In the present paper, we leverage the concepts presented in [7] and propose an approach for extracting the complex frequency response of a sampling oscilloscope using a calibrated LSNA to calibrate a broadband pulse at the reference plane of the oscilloscope.

The key points of our approach include: 1) the reference pulse source does not need to be pre-characterized, 2) the measurements are performed without disconnecting the measurement instruments, 3) oscilloscope match measurement is not required, 4) as a consequence of 2 and 3, the impact of drift and measurement uncertainty is reduced, 5) This approach provides a convenient way of traceably transferring NIST EOS absolute phase and calorimetric power to sampling oscilloscopes using a calibrated LSNA.

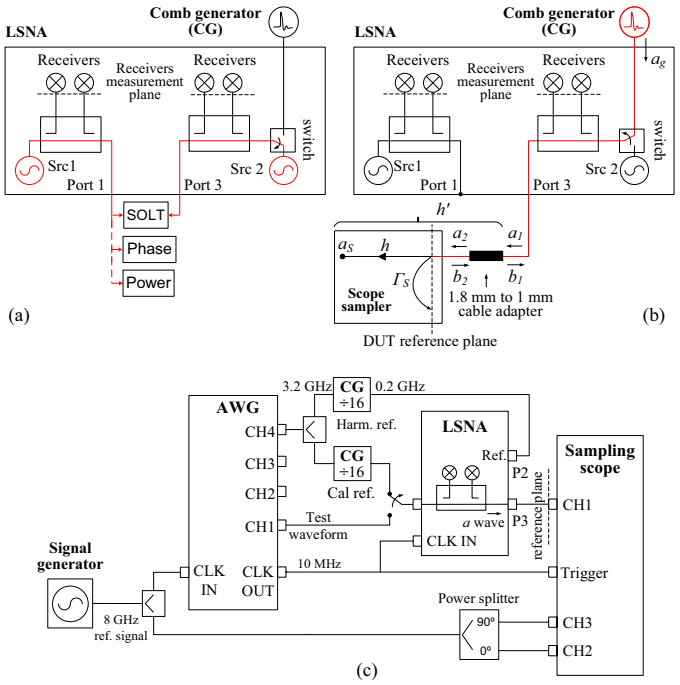

Fig. 1 a) LSNA calibration setup. b) Setup used during the scope characterization. c) Illustration of the measurement synchronization scheme.

II. Measurement Setup

The measurement setup is shown in Fig. 1. First, the LSNA was calibrated using its internal continuous wave (CW) sources (Fig. 1a). Afterward, the LSNA source on port 3 was replaced with an external comb generator during the scope characterization experiment (Fig. 1b) and with an arbitrary waveform generator (AWG) during the validation measurements (Fig. 1c). In both cases, the external signal was passed through the LSNA test set and fed into the oscilloscope through the LSNA test port 3.

Passing the signal of interest through the LSNA test set allows us to perform the LSNA and oscilloscope measurements without disconnecting the instruments, which reduces drift and measurement uncertainty related to cable movement and connector repeatability.

Synchronization is key in this experiment, as all equipment including the LSNA (Keysight PNA-X N5245A[1]), sampling oscilloscope (Keysight sampling head 86118A), phase references (Keysight comb generators U9391F) and AWG (Keysight M8195A) must be locked to the same reference signal (see Fig. 1c). An 8 GHz sine-wave signal generated by an external signal generator was used as the master reference signal to which all the others were locked.

In addition to generating validation test signals on channel 1, the AWG synchronously triggers the sampling oscilloscope and clocks the LSNA through its 10 MHz output clock and drives the comb generators with a 3.2 GHz signal generated on channel 4.

An in-phase and quadrature (IQ) signal derived from the 8 GHz reference was measured by the oscilloscope simultaneously with the waveform of interest. This signal was used in the NIST Time-Base Correction (TBC) algorithm to correct for jitter and other time-base distortions in the oscilloscope-measured signal [8].

III. Complex Frequency Response Characterization

A. LSNA calibration and measurements

The two-step procedure used to perform calibrated LSNA measurements with an external source is illustrated in Fig. 1:

1. First, we operated the LSNA in the default configuration using its internal CW sources, and performed short-open-load (SOLT), absolute amplitude and absolute phase calibrations (Fig. 1a).
2. Then, with the sampling oscilloscope connected to the LSNA front test port 3, we routed that port to the LSNA back-panel connector, where a 50 GHz bandwidth comb generator was connected during the oscilloscope characterization, and a 65 GSample/s, 20 GHz bandwidth AWG was connected during the validation measurements (see Fig. 1b and 1c). Note that changing the source configuration does not affect the calibration performed in step 1, as the full-wave calibration is independent of the source [9].

We measured 0.2 GHz and 1 GHz harmonic signals. For the 0.2 GHz signals, we used a 0.2 GHz to 50 GHz measurement grid with a step of 0.2 GHz, and for the 1 GHz signals, we used a 1 GHz to 50 GHz measurement grid with a step of 1 GHz. For both measurements, we drove the comb generators with a 3.2 GHz signal generated on the AWG channel 4 and we set their divide ratios to 16, defining a frequency resolution of 0.2 GHz.

B. Deriving the oscilloscope complex frequency response

First, we applied the NIST TBC algorithm [8] to the oscilloscope raw data to correct for time-base distortion, using the IQ signal measured on channels 2 and 3, and we interpolated the corrected waveform to a uniform time grid.

After calibrating the LSNA data (referenced to the input of the cable adapter, Fig. 1b[2]), we derived the complex frequency response of the oscilloscope plus cable adapter cascade, h'. This was done in the frequency domain by dividing the Fourier transform of the TBC-corrected oscilloscope signal, a_{s}, by the calibrated LSNA signal, $a_{1\mathrm{LSNA}}$ (1).

Afterward, we used (2) to de-embed the cable adapter and find the oscilloscope frequency response, h. De-embedding the cable adapter was necessary to compare our results to the previous NIST characterization [5], which is referenced to the input of the oscilloscope sampling head (without the cable adaptor).

In addition, we defined a scaling factor, α, to amplitude-normalize the NIST characterization, h_{NIST}, to the amplitude of the LSNA fundamental component measured here (3).

$$h'(\omega) = \frac{a_{\mathrm{s}}(\omega)}{a_{1\mathrm{LSNA}}(\omega)} \tag{1}$$

$$h(\omega) = h'(\omega)\frac{1-\Gamma_{\mathrm{S}}(\omega)S_{22}(\omega)}{S_{21}(\omega)}$$

$$= h'(\omega)\left(S_{21}(\omega) + S_{22}(\omega)\frac{b_1(\omega) - a_1(\omega)S_{11}(\omega)}{a_1(\omega)S_{12}(\omega)}\right)^{-1} \tag{2}$$

$$\alpha = \frac{|h(\omega_0)|}{|h_{\mathrm{NIST}}(\omega_0)|} \tag{3}$$

where $a_{1\mathrm{LSNA}}$ is the LSNA calibrated measurement, a_s is the oscilloscope data (after TBC-correction), S_{21} and S_{22} are measured scattering parameters of the cable adapter and Γ_{S} is the measured reflection coefficient of the oscilloscope sampling head. Since LSNA-calibrated measurements of a_1 and b_1 are available, using the right side of (2) to de-embed the cable adapter avoids the uncertainty in a separate measurement of Γ_{S}.

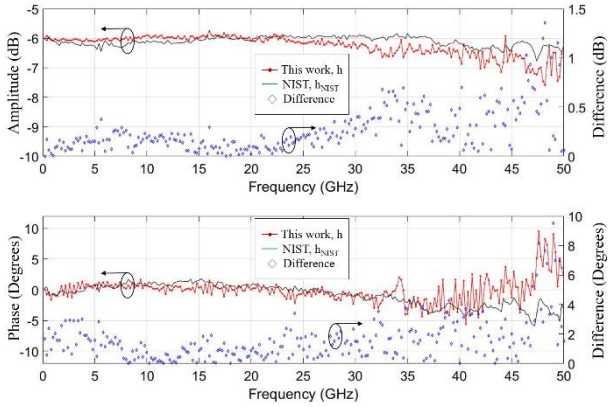

Fig. 2 Frequency response of Keysight sampling head 86118A obtained in this work and previously obtained by NIST.

[1] We specify brand names only to better explain the experiments. NIST does not endorse commercial products. Other products may perform as well or better.

[2] A 1.85 mm to 1 mm cable adapter was required to interconnect the 2.4 mm LSNA to a 1 mm connector attached to the oscilloscope sampling head.

IV. Measurement Results

A. Extracting the oscilloscope complex frequency response

The comb generator used in our experiment has low amplitude compared to the dynamic range of the measurement instruments. Furthermore, the LSNA that we used presents a large back-to-front panel insertion loss. As such, the signal-to-noise ratio (SNR) of the comb waveform measurement is degraded when the signal is passed through the LSNA test set, especially at higher frequencies.

This was evaluated in [7], where it was also found that this LSNA presents lower insertion loss at port 3 (14 dB at 50 GHz) compared to port 1 (22 dB at 50 GHz). For that reason, we used port 3 in this experiment.

To further improve the measurement quality: 1) we reduced the LSNA IF bandwidth to 3 Hz and averaged 10 measurements of the calibration phase reference and 28 measurements of the test comb generator. 2) we corrected the time-base of the oscilloscope for jitter and time-base distortion and we averaged 1000 oscilloscope measurements.

Fig. 2 shows the frequency response of the Keysight sampling head 86118A obtained in this work and previously obtained by NIST, up to 50 GHz. The NIST frequency response was normalized to the LSNA fundamental amplitude using the scaling factor α. We achieved less than 0.7 dB amplitude difference and less than 5 degrees phase difference up to 45 GHz.

B. Validating the proposed approach

To validate our procedure, we replaced the comb generator used during the oscilloscope characterization with an AWG, which was used to generate several test signals, including a 200 MHz square wave, a 1 GHz square wave and a 1 GHz pulse repetition rate sinc-like waveform. We measured these signals with the LSNA, we calibrated them and translated them to the reference plane of the sampling oscilloscope.

Without disconnecting the instruments, we measured the same signals with the sampling oscilloscope and we corrected for jitter and time-base distortion. Afterward, we corrected for the frequency response of the oscilloscope obtained in this work, h, and previously obtained by NIST, h_{NIST}. Finally, we time-aligned all the waveforms by phase-normalizing them to their fundamental components. The results, presented in Fig. 3, display excellent agreement.

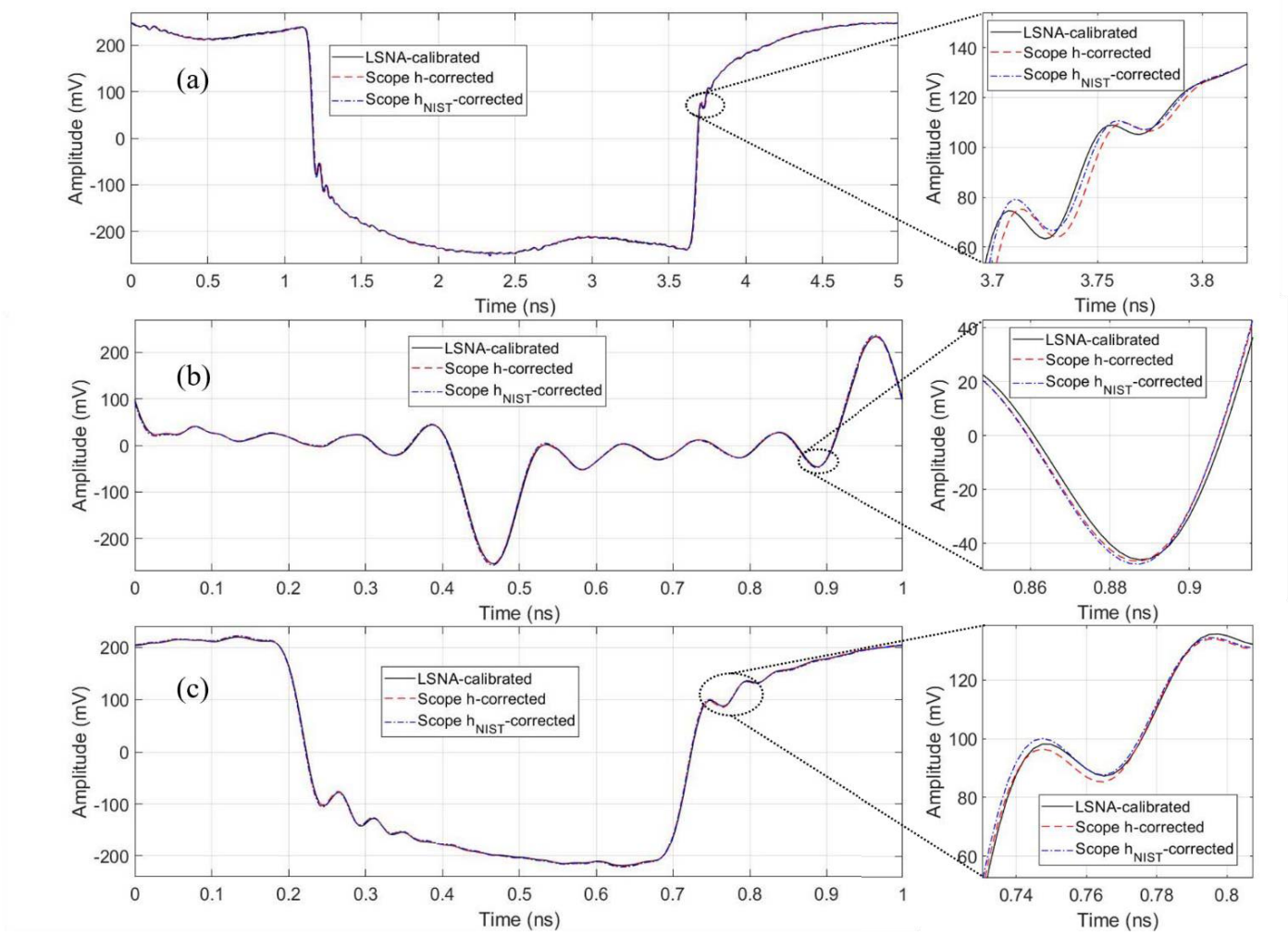

Fig. 3 Reconstructed incident wave at the oscilloscope input, calibrated with the LSNA and corrected for the oscilloscope frequency response obtained in this work and previously obtained by NIST. a) 200 MHz square wave, b) 1 GHz sinc-like waveform, c) 1 GHz square wave.

V. Conclusion

We proposed a new approach for characterizing the complex frequency response of sampling oscilloscopes that enables traceable standards transfer through a calibrated LSNA. We showed good agreement between our results and previous NIST results, typically less than 0.7 dB amplitude and 5 degrees phase difference up to 45 GHz.

As an alternative to the use of an external broadband source to characterize the oscilloscope, the internal LSNA CW source could be swept across the bandwidth of interest. However, using an external broadband source significantly reduces the oscilloscope measurement time, as the signal is acquired in the time-domain in a single take. Furthermore, cross-frequency phase-coherence is desired in some applications [10].

Improvements to our setup and procedure may include the use of external couplers to improve the SNR of the LSNA measurements and the use of a two-tier calibration approach that includes the cable adapter.

References

[1] D. Williams et al., "The Sampling Oscilloscope as a Microwave Instrument," *IEEE Microwave Mag.*, vol. 8, no. 4, pp. 59-68, Aug. 2007.

[2] K. A. Remley *et al*., "Millimeter-Wave Modulated-Signal and Error-Vector-Magnitude Measurement With Uncertainty," in *IEEE Transactions on Microwave Theory and Techniques*, vol. 63, no. 5, pp. 1710-1720, May 2015.

[3] D. F. Williams *et al*., "Sampling-oscilloscope measurement of a microwave mixer with single-digit phase accuracy," in *IEEE Transactions on Microwave Theory and Techniques*, vol. 54, no. 3, pp. 1210-1217, March 2006.

[4] D. Henderson et al., "Recent developments in the calibration of fast sampling oscilloscopes," *IEE Proc*., vol. 139, no. 5, pp. 254–260, Sept. 1992.

[5] T. S. Clement, et al., "Calibration of sampling oscilloscopes with high-speed photodiodes," *IEEE Transactions on Microwave Theory and Techniques*, vol. 54, no. 8, pp. 3173-3181, Aug. 2006.

[6] Fuser H. et al. "Optoelectronic time-domain characterization of a 100 GHz sampling oscilloscope", Meas. Science and Tech., 2012. 23 1–10.

[7] Alirio Boaventura et al., "Traceable Characterization of Broadband Pulse Waveforms using a Large Signal Network Analyzer and a Sampling Oscilloscope", IMS 2018, Pennsylvania, June 2018.

[8] P. D. Hale et al., "Compensation of Random and Systematic Timing Errors in Sampling Oscilloscopes," *IEEE Trans. on Inst. and Meas.*, vol. 55, no. 6, 2146-2154, Dec. 2006.

[9] Valeria Teppati, Andrea Ferrero and Mohamed Sayed, "Modern RF and Microwave Measurement Techniques", Cambridge University Press, Cambridge UK, July 2013.

[10] D. Kim et al. "Traceable calibration for a digital real-time oscilloscope with time interleaving architecture", Meas. Science and Tech., 29 015003, 2018.